Seventh Framework Programme
Theme 9 Space FP7-SPA.2009.1.1.02
Monitoring of climate change issues (extending core service activities)

Grant agreement for: Collaborative Project (generic).
Project acronym: **MONARCH-A**
Project title: **MONitoring and Assessing Regional Climate change in High latitudes and the Arctic**
Grant agreement no. 242446
Start date of project: 01.03.10
Duration: 36 months
Project coordinator: Nansen Environmental and Remote Sensing Center, Bergen, Norway

D1.5.1: Software modules interfacing variables derived in WP 1.1-1.4 to models.

Software modules interfacing variables derived in WP 1.1-1.4 to selected coupled carbon, water and climate models.

Due date of deliverable: 31.08.2012

Actual submission date: 04.09.2012

Organization name of lead contractor for this deliverable: USFD

Project co-funded by the European Commission within the Seventh Framework Programme, Theme 6 Environment		
Dissemination Level		
PU	Public	X
PP	Restricted to other programme participants (including the Commission)	
RE	Restricted to a group specified by the consortium (including the Commission)	
CO	Confidential, only for members of the consortium (including the Commission)	

ISSUE	DATE	CHANGE RECORDS	AUTHOR
0			

SUMMARY

Essential Climate Variables (ECV) data sets collected during the 1st phase of Work Package 1 (WP1) in Monarch-A are used to drive and assess land surface models with the aim of improving their accuracy and identifying uncertainty hotspots. The ECVs used for this purpose are: Land Cover, Burned Area, Permafrost and Snow Variables, all of which were collected for the purpose of deliverables during the 1st phase of WP1.

Exploiting the information contained in these datasets involved modifications to both the datasets and the models. In some cases it was simply converting data to the format and geometry used by the models, but in most cases some form of transformation was needed to convert data into forms that were consistent with the models. For example, the Land Surface Models contained in climate models use a simplified parameterised description of vegetation (Plant Functional Types) and the existing land cover ECVs need to be converted to this form for use or comparison with models. Comparisons between models and ECV datasets in many cases revealed that the models contained poor representations of physical processes, and this involved modifications to the models themselves.

A proper understanding of data-model interface issues requires substantial background, and such a detailed account is best given in the context of other deliverables, such as D1.4.1: "Analysis of available land cover and fire products and recommendations for use in climate models" and D1.4.2: "Land cover maps transformed into forms suitable for climate modelling". This report therefore gives only a brief summary of key interface issues and describes some of the consequences of providing such interfaces. In particular, it is shown that: a) uncertainties in ECVs that drive a model can be transferred into uncertainties in modelled carbon fluxes; b) statistical characteristics of ECVs extracted from their time series can improve model performance; and c) agreement of model outputs with reference ECV data sets does not guarantee the validity of embedded model processes.

MONARCH-A CONSORTIUM

Participant no.	Participant organisation name	Short name	Country
1 (Coordinator)	Nansen Environmental and Remote Sensing Center	NERSC	NO
2	The University of Sheffield	USFD	UK
3	Universität Hamburg	UHAM	NO
4	Centre National de la Recherche Scientifique	CNRS	FR
5	Scientific foundation Nansen International Environmental and Remote Sensing Center	NIERSC	RU
6	Universitetet i Bergen	UiB	NO
7	Danmarks Tekniske Universitet	DTU	DK
8	Institut Francais de Recherche pour l'Exploitation de la Mer	IFREMER	FR

Table of Contents

List of Figures

List of Tables

No table of figures entries found.

1 Introduction

It has been demonstrated that the main source of uncertainty in predictions for the next 30 years is the lack of adequate information on initial conditions, whereas beyond that it arises from errors in climate model formulation and parameterization [*Cox and Stephenson*, 2007]. Several initiatives to address the initial value problem have taken place over the past years, such as the establishment of Essential Climate Variable (ECV) datasets under the framework outlined by the Global Climate Observing System [*GCOS*, 2004; 2010].

In a similar approach, the first phase of Work Package 1 (WP1) in MONARCH-A included deliverables that mainly involved the collection, amalgamation and assessment of ECV datasets relevant to northern latitudes, such as permafrost distribution, land cover and snow characteristics like snow depth and density. A variety of sources was used, including active & passive remote sensing as well as ground reference data.

The second phase, part of which represents the present deliverable, is to interface the ECV datasets to land surface models. This can be achieved by comparing model outputs with the relevant ECVs, by forcing/driving the models using the ECV datasets as input drivers, by using the data to optimize model parameters, or by full data assimilation. In all cases, the goal is to improve model accuracy and quantify how the uncertainty in key variables at pan-boreal latitudes is transferred to calculations of carbon and water fluxes provided by the models.

2 Methodology

Here we present a list with the ECVs examined during MONARCH-A in WP1, the methodologies followed to interface them with a set of land surface models, and conclusions. As the different ECVs relate to different processes it was not possible to follow a single methodology which would simplify the process; instead a different approach was followed for each ECV and details will be given when each variable is presented.

2.1 Land Cover

A source of uncertainty in model estimates of Net Biome Production (NBP), fire emissions and water fluxes is land cover. Most land surface models require land cover maps as inputs in order to determine the characteristics of the overlaying vegetation and apply the appropriate physical processes. These maps usually originate from classification of Earth Observational data sets and the four most widely used are: GlobCover [*Arino et al.*, 2008], GLC2000 [*Bartholome and Belward*, 2005], MODIS LC [*Friedl et al.*, 2010] and the Vegetation Continuous Field (VCF) product derived from MODIS [*Hansen et al.*, 2003]. In order to interface these land covers into a land surface model 3 modifications are required:

a) Reduction in spatial resolution: although for many applications a high spatial resolution land cover dataset is desired, climate models adhere to the resolution of their climate drivers, which is relatively poor and usually within 0.5°-1°. In contrast, global satellite-derived land covers follow the resolution of the sensor they were derived from, and in general the finished products are offered at resolutions of a few hundred meters to a kilometer (GlobCover-300m, GLC2000-0.009°, MODIS LC-0.05° and MODIS VCF-0.0045°). Hence a first requirement for interfacing these products to the models was to utilize FORTRAN image resizing subroutines to reduce their resolution to 0.5° - 1°.

b) Change of file format: the remote sensing community that produces the land cover data sets prefers to distribute their products as image files. On the other hand, land modelers require essential meta-data information so they prefer file formats such as NetCDF and HDF, which is why the majority of land model codes require the driver files to follow such formats. So the second step was to use Matlab and FORTRAN subroutines to convert the image land cover files into NetCDF file format.

c) Land class conversion: even though land cover products follow certain classification rules (e.g. [*GCOS*, 2010]), the classes used are not explicitly defined so differ between products, while surface models use their own classes or Plant Functional Types (PFTs) to assign different characteristics to

vegetation. It is thus necessary to translate surface classes from land cover classifications into model-specific PFTs. This can be achieved by following the class description from the classification and assigning appropriate relative weights to each PFT. More details on the particular methodology are given in the deliverable D1.4.2: 'Land Cover Maps Transformed into Forms Suitable for Carbon, Water & Climate Modeling'.

A source of uncertainty in model estimates of Net Biome Production (NBP), fire emissions and water fluxes is land cover, and during processing of the land cover data sets it was established that they exhibit great differences (Fig. 1 (top)). To evaluate the effects of these differences and the uncertainties they impose on the resulting carbon fluxes of a land surface model we used the 4 land cover datasets mentioned above to drive the Sheffield Dynamic Global Vegetation Model (SDGVM) [*Woodward et al.*, 1995]. The resulting average fluxes making up the carbon balance of the pan-boreal region over the period 1981-2006 are presented in Fig. 1 (bottom). Despite large differences in the proportions in the three generic land cover types (tree, herbaceous and bare cover) in the land cover maps (Fig. 1 (top)), Net Primary Productivity (NPP) and Heterotrophic Respiration (R_h) show differences of only a few per cent between the various land covers. Larger differences occur in Net Ecosystem Production (NEP) and fire emissions. Since SDGVM treats only above-ground biomass as fuel, fire emissions are roughly linearly proportional to tree cover, so the largest difference is between GLC2000 (40% tree cover) and MODIS VCF (25% tree cover), with the latter giving almost 50% lower emissions. NBP for pan-boreal latitudes was found to be well-approximated (adjusted R^2 = 0.69) by a linear function of tree and grass cover given by:

$$NBP = 6.82(\pm 1.96) \times (\text{Tree Cover}) + 2.98(\pm 1.31) \times (\text{Grass Cover})$$

with NBP in units of 10^{14} gC yr^{-1} and cover expressed as a fraction between 0 and 1. This leads to differences of 20% between the lowest carbon uptake (GlobCover) and highest (GLC2000); GlobCover has the highest fraction of bare ground, while GLC2000 has the least bare ground and the highest amount of tree cover.

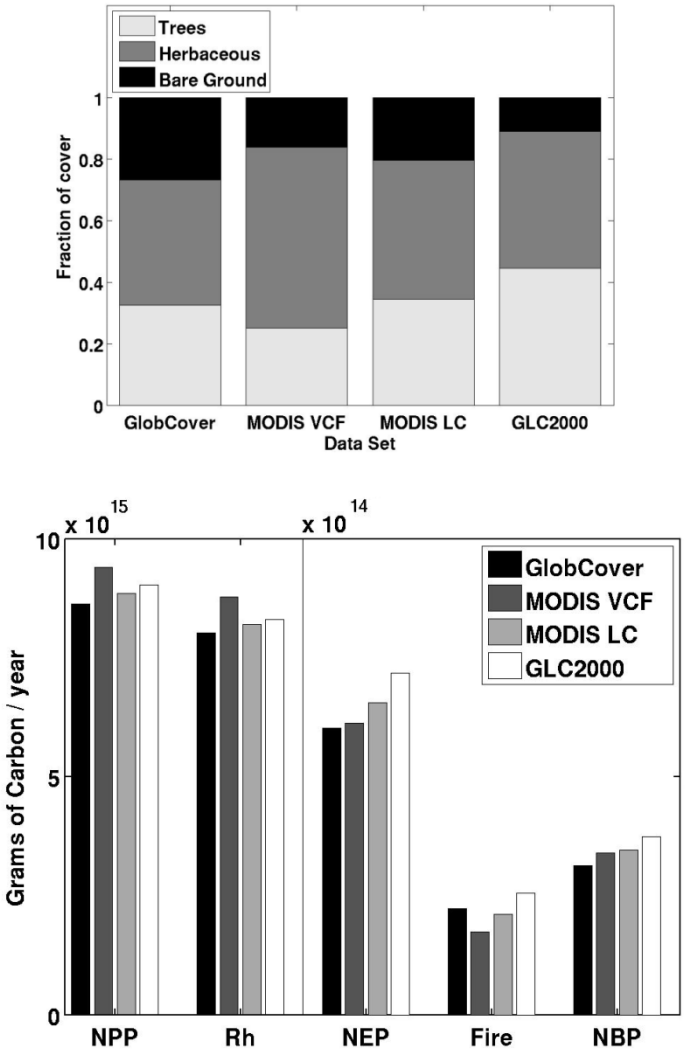

Figure 1: (top) Pan-boreal fractions of three generic cover types (trees, herbaceous cover and bare ground) derived from the four land cover maps. (bottom) Average values of pan-boreal NPP, R_h, NEP, fire emissions and NBP calculated by SDGVM over the period 1981-2006 when driven with GlobCover, MODIS VCF, MODIS LC and GLC2000.

No significant differences were found in water fluxes (runoff and evapotranspiration) when SDGVM was driven by GLC2000, MODIS LC and MODIS VCF (Fig. 2); more details can be found in deliverable D1.4.1: 'Analysis of available land cover and fire products, their trends and uncertainties, preferred products, and recommendations for combining different products for best use in climate models'.

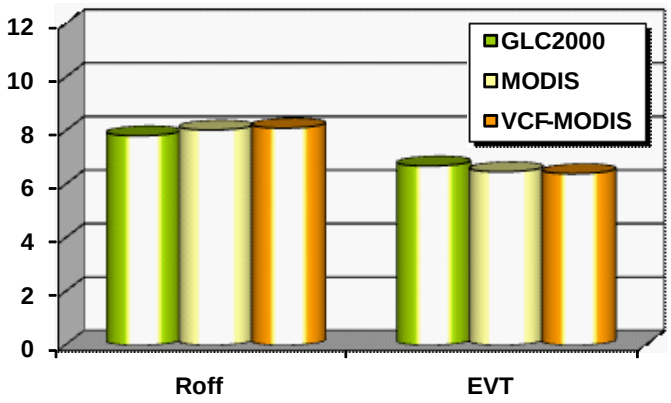

Figure 2: SDGVM water fluxes for GCL2000, MODIS and VCF-MODIS (Tt y^{-1}).

2.2 Fire

Comparison of model outputs of burned area with EO data (the Global Fire Emissions Database-Burned Area, [*van der Werf et al.*, 2010]) collected for deliverable D1.4.1: 'Analysis of Available Land Cover & Fire Products' revealed that modeled burned area had significantly less inter-annual variability (IAV) than the observations. The effects were investigated by modifying SDGVM so as to force the calculated IAV of burned area to be consistent with that observed in GFED-BA (Fig. 2).

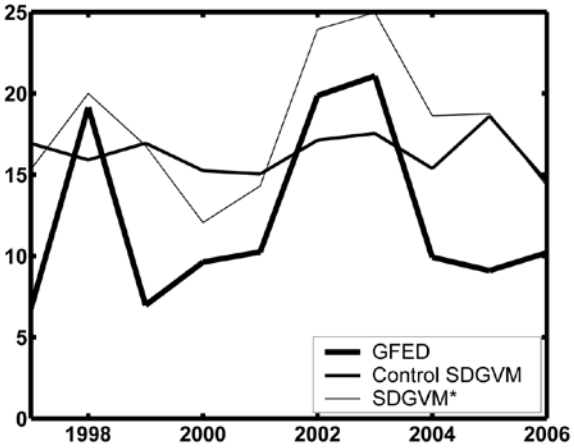

Figure 3: Burned area (in Mha) from GFED-BA, SDGVM and the SDGVM with the adjusted burnt area (denoted as SDGVM) for the pan-boreal region for 1997-2006.*

Shown in Fig. 3 are time series (1960-2006) of the de-trended NBP (lower plot) and fire emissions (upper plot) calculated by SDGVM and SDGVM*. As expected, the inter-annual variability of the fire emissions increases significantly as a result of the increased variability in burnt area. However, the

inter-annual variability of NBP is not significantly affected, and there is little correlation between NBP and the size of the emissions. Although the variance of the NBP in the adjusted run increased by 15.0%, only 22% of the adjusted NBP variance can be attributed to the variance of the adjusted fire emissions; this is insufficient to affect the sign of the NBP and turn a sink year into a source and vice versa. Although the IAV of the burnt area now corresponds much more closely to that of the observations, the mean behavior and trends of burnt area, emissions and NBP are unaffected. In other words, for the pan-boreal region, fire emissions are not the major driver of the observed variability of land-atmosphere carbon exchange. This is consistent with the finding of [*Prentice et al.*, 2011] that (at global scale) during 1997-2005, the CO_2 fluxes produced by GFED would have contributed only a third of the variability in total CO_2 flux inferred from atmospheric inversion, despite earlier studies postulating that biomass burning contributes greatly to land-atmosphere carbon flux anomalies [*Nevison et al.*, 2008; *Patra et al.*, 2005]. In the case presented here, fire emissions contribute around 22% of the variability of the CO_2 flux. More details can be found in deliverable D1.4.3: 'Integrated Fire Products for Carbon & Climate Modeling'.

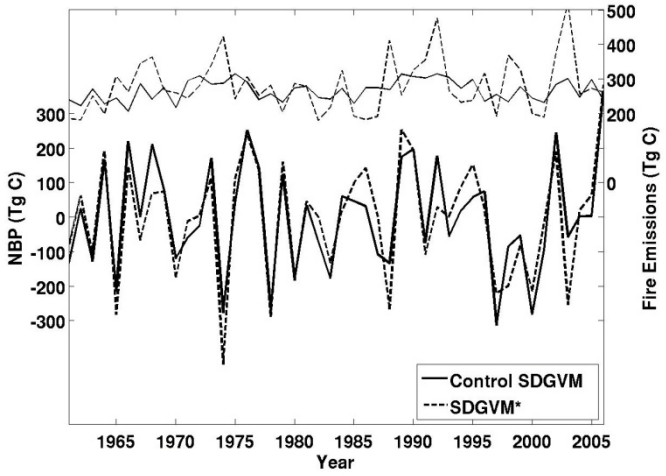

Figure 4: Time series (1960-2006) of the de-trended NBP (solid lines, left y-axis) and fire emissions (dashed lines, right y-axis) for SDGVM and its modified version, SDGVM.*

Furthermore, we modified the fire disturbance in LPJ-WM model to follow the statistical characteristics of reference data and specifically GFED-BA, a dataset containing monthly burned area on a global scale with a 0.5° resolution. Details are not presented in this document as an extensive description of the methodology can be found in the Deliverable D1.4.3: 'Integrated Fire Products for Carbon and Climate Modeling'. Briefly stated, the LPJ-WM fire process was altered to give burnt area statistical properties that more closely resemble the GFED-BA data, but without changing the mean

area burnt by the model. This was achieved by deriving the cumulative distribution function (CDF) of the annual fraction burnt per disturbed grid cell from GFED-BA, and forcing LPJ-WM to obey the same distribution; this modified version of LPJ-WM will be denoted as LPJ-WMa. At the 0.5° resolution of GFED-BA, the CDF of annual fraction burnt area per disturbed grid cell for boreal latitudes over the period 1997-2009 was found to be well approximated by a gamma distribution of form:

$$p(X \le x) = \frac{1}{b^a \, \Gamma(a)} \int_0^x t^{a-1} \, e^{-t/b} \, dt$$

with parameters a = 0.21 and b = 0.1 and expected value of 0.021. Fig.5 shows the observed CDF and that produced by LPJ-WMa over the same period and spatial subset. Note that the CDF will normally depend on the resolution of the dataset used to produce it.

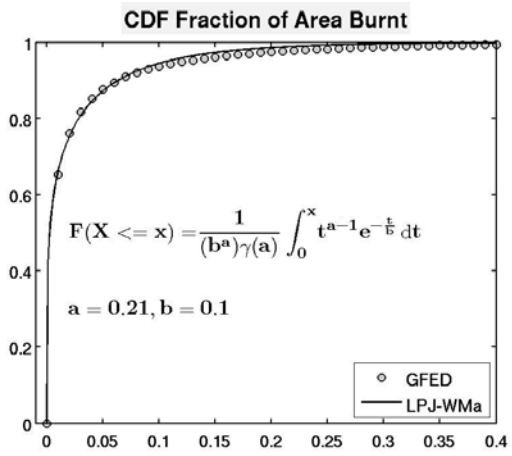

Figure 5: CDF of fractional annual burnt area per disturbed grid cell for GFED-BA and LPJ-WMa. On average, GFED-BA indicates about 8% of grid cells to be disturbed each year. Values with percentage burnt area exceeding 40% have probability less than 0.0012 so are omitted from the CDF plot.

This methodology offers a more realistic fire regime for the model, but LPJ-WM still lacks a radiative transfer model to describe the input radiation flux at the top of the snow/soil interface; this provides necessary boundary conditions for the atmosphere-soil heat exchange. This omission is crucial because, as stated in Deliverable D1.4.3, a further effect is that removal of canopy by fire alters the radiation budget: for example, prior to disturbance, 30-65% of incoming solar radiation reaches the forest floor in black spruce forests [*Slaughter*, 1983], while after a fire it exceeds 90% [*Kasischke et al.*, 1995]. This effect cannot be simulated by the current version of LPJ-WM, which lacks a full radiation balance in the energy calculations. Hence an approximation was made in which

the input air temperature, which acts as an upper boundary condition for the heat diffusion equation, was increased in the year after a fire and decreased as an exponential function of tree cover. This simulates an increase of Leaf Area Index and associated attenuation of radiation according to Beer-Lambert's Law.

The cumulative effect of these two modifications is illustrated by Fig.6, in which the upper plot shows the monthly soil temperatures at depth of 10 cm calculated by LPJ-WMa at a location dominated by deciduous needle-leaved forest in northern Siberia after a fire with 99% fraction of burn. Following the disturbance, the model initially sets herbaceous cover as the dominant PFT in the grid-cell, while the needle-leaved PFT becomes dominant after 15 years. Fig. 6 shows that the removal of litter and its subsequent damping effect increases the monthly variability of soil temperature as it becomes more susceptible to air temperature and its periodic fluctuations. Since summer soil temperatures now exceed 0° C, summer thaw depth increases by over 1.0 m and requires more than 60 years to return to its pre-disturbed value; this is more consistent with field data than when the boundary conditions were unchanged, in which case the increase in maximum thaw depth due to loss of litter is less than 0.5 m, although the time to recovery of the original temperature conditions is the same (see Fig. 6).

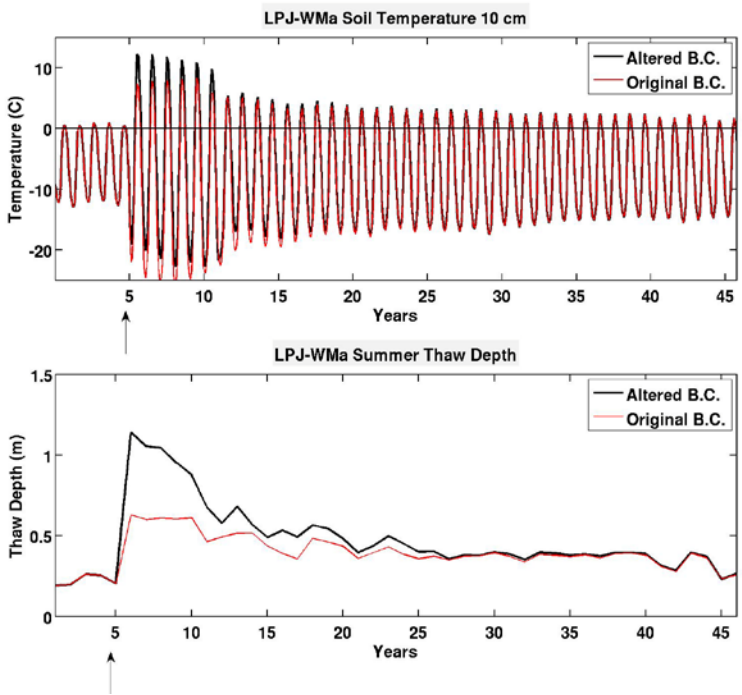

Figure 6: (top) Monthly soil temperatures for altered and original boundary conditions (B.C.) at depth of 0.1 m produced by LPJ-WMa at a site which experienced more than 99% of burn; the arrow marks the year of the fire disturbance. (bottom) Thaw depth averaged over summer months for the same sites.

2.3 Permafrost

For the purposes of the deliverable D1.3.1: 'Reference Permafrost Map from Historical Sources' a digital map of the permafrost extent over northern latitudes was produced using a variety of sources, including digitization of a large number of permafrost maps printed in the 1980s in the former Soviet Union. This information was used to assess the accuracy of the permafrost extent in the LPJ-WM land surface model and results showed that the model performs well in capturing the permafrost boundaries both in N. America and Eurasia (Fig. 7). However, an error was found in the LPJ-WM code which caused some important variables to attain unrealistic values. In particular, the error caused the depth of the litter layer to decouple from the amount of carbon found in the litter layer, e.g. a grid cell with several kg/m^2 of carbon in its soil column would be represented by a default depth of 5 cm. This error affects about half of the grid cells in the boreal latitudes and when corrected the soil temperature changed by ±1-7°C depending on location and time of year. Obviously the model needs a new parameterization and we are currently in correspondence with the author about releasing a new version. It is interesting to note that the model had been parameterized so that the permafrost extent showed good agreement with reference data despite the error; hence agreement with data does not guarantee model correctness. In the context of permafrost-fire feedbacks the reader is referred to Deliverable D1.3.3: 'Model for energy flows in permafrost/soil /snow/atmosphere layered media interfaced to the BCM climate model' where an extended discussion of this issue is described.

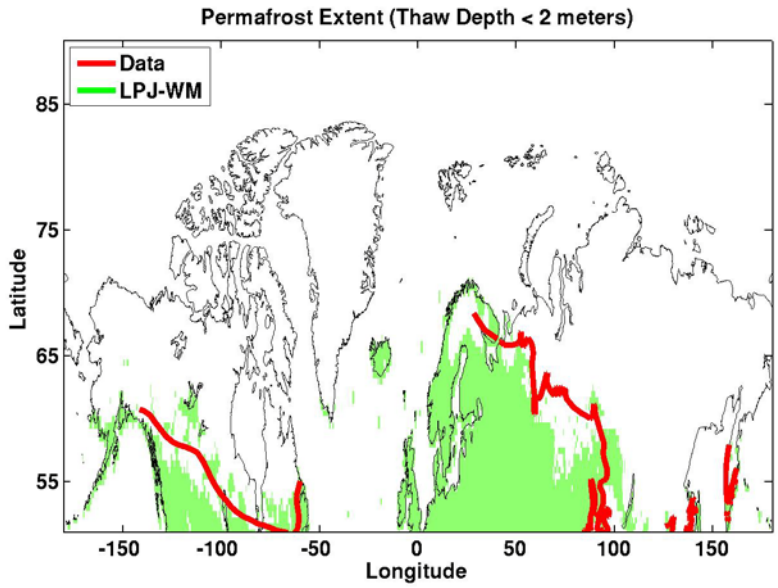

Figure 7: Comparison of the permafrost extent over the boreal latitudes between the LPJ-WM land model and data from a variety of reference sources amalgamated for the purposes of the deliverable D1.3.1.

2.4 Snow Variables

In situ observations can be used to optimize model parameters linked to a certain variable output by the model by minimizing an error function that describes the difference between the modeled and observed values of the variable. Following this methodology we are using in situ snow water equivalent (SWE) field data [*Krenke*, 2004] and the JULES land surface model to optimize SWE output from JULES. JULES was chosen as it has a large set of well-defined parameters which are easily accessible through its input files. An off-the-shelf optimization (the downhill simplex method in multi-dimensions from Numerical Recipes in Fortran [*Perrin*, 1997]) is being used to perform a feasibility study as to whether the model can be successfully optimized and, if so, what will be the effect on model calculations of snow and runoff from snow-melt.

The error function was defined as the average absolute difference in monthly snow season SWE per site, and a set of 9 parameters was chosen for optimization. These parameters were selected by the criterion that they are most likely to influence SWE: an example is initial snow density. The algorithm was modified to allow sensible constraints to be applied to these parameters; each parameter was constrained to lie between 50% and 200% of its original value.

JULES is relatively CPU intensive, since it uses a 6-hour time-step and the WATCH climate database that drives the model is large, with 64,000 sites. Initial results are not encouraging as the error function appears to be very insensitive to changes in parameters, and we are currently checking whether this is a coding error or an intrinsic property of the system.

3 Conclusions

Effective use of any of the land ECVs considered in MONARCH-A involved modifications to the datasets, or the Land Surface Models, or both. Although some of the modifications were relatively straightforward (e.g., geometric and coordinate system conversions), in some cases the ECV data revealed glaring weaknesses in the ways models represented key processes, and these involved significant changes to the model themselves.

It is not appropriate in this summary document to give a detailed account of all interface issues: that is best done in other deliverables where the full context of the links between models and data can be explained. Instead in the current deliverable we have summarised key interface issues and illustrated some of the consequences that flow from establishing such links between land surface models and ECVs. In particular, we identify three major generic conclusions:

a) When ECVs are used as drivers, the uncertainty in model calculations is linked to the uncertainty contained in the ECVs. This is clearly demonstrated in the case of land cover, where differences in the land cover data sets translate into significant differences in the fire emissions and NBP produced by the models.

b) Constructing time series of ECVs offers insights into their statistical properties, and these can be used to modify models and improve their performance. This was demonstrated by using time series of the burned area ECV to learn its inter-annual variability (IAV). The SDGVM model was then constrained to produce a similar IAV, and its outputs were examined to understand the consequences for NBP and other carbon fluxes behave under these more realistic conditions. Additionaly, by extracting the Cumulative Distribution Function of the annual area burned in a grid cell we acquired a more realistic fire regime for the boreal latitudes which was forced in LPJ-WM and provided useful insights on fire-permafrost interactions.

c) Our analysis of the LPJ-WM model showed that it gave good agreement in permafrost extent when compared with data despite a serious coding error which led to non-physical variable values. This illustrates that agreement between model outputs an ECV data does not guarantee the validity of the underlying model processes.

4 References

Arino, O., P. Bicheron, F. Achard, J. Latham, R. Witt, and J. L. Weber (2008), GLOBCOVER The most detailed portrait of Earth, *Esa Bull-Eur Space*(136), 24-31.

Bartholome, E., and A. S. Belward (2005), GLC2000: a new approach to global land cover mapping from Earth observation data, *Int J Remote Sens*, *26*(9), 1959-1977, doi: 10.1080/01431160412331291297.

Cox, P., and D. Stephenson (2007), Climate change - A changing climate for prediction, *Science*, *317*(5835), 207-208, doi: 10.1126/science.1145956.

Friedl, M. A., D. Sulla-Menashe, B. Tan, A. Schneider, N. Ramankutty, A. Sibley, and X. M. Huang (2010), MODIS Collection 5 global land cover: Algorithm refinements and characterization of new datasets, *Remote Sens Environ*, *114*(1), 168-182, doi: 10.1016/j.rse.2009.08.016.

GCOS (2004), Implementation plan for the Global Observing System for Climate in support of the UNFCCC, GCOS–92, WMO Technical Document No. 1219, Geneva, WMO.

GCOS (2010), Implementation Plan for the Global Observing System for Climate in Support of the UNFCCC (2010 Update), WMO.

Hansen, M. C., R. S. DeFries, J. R. G. Townshend, M. Carroll, C. Dimiceli, and R. A. Sohlberg (2003), Global Percent Tree Cover at a Spatial Resolution of 500 Meters: First Results of the MODIS Vegetation Continuous Fields Algorithm, *Earth Interact*, *7*.

Kasischke, E. S., N. L. Christensen, and B. J. Stocks (1995), Fire, Global Warming, and the Carbon Balance of Boreal Forests, *Ecol Appl*, *5*(2), 437-451.

Krenke, A. (2004), Former Soviet Union hydrological snow surveys, edited, NSIDC, Boulder,CO.

Nevison, C. D., N. M. Mahowald, S. C. Doney, I. D. Lima, G. R. Van der Werf, J. T. Randerson, D. F. Baker, P. Kasibhatla, and G. A. McKinley (2008), Contribution of ocean, fossil fuel, land biosphere, and biomass burning carbon fluxes to seasonal and interannual variability in atmospheric CO(2), *J Geophys Res-Biogeo*, *113*(G1), doi: 10.1029/2007jg000408.

Patra, P. K., M. Ishizawa, S. Maksyutov, T. Nakazawa, and G. Inoue (2005), Role of biomass burning and climate anomalies for land-atmosphere carbon fluxes based on inverse modeling of atmospheric CO2, *Global Biogeochem Cy*, *19*(3), doi: 10.1029/2004gb002258.

Perrin, C. L. (1997), Numerical recipes in Fortran 90: The art of scientific computing, second edition, volume 2, *J Am Chem Soc*, *119*(37), 8748-8748.

Prentice, I. C., D. I. Kelley, P. N. Foster, P. Friedlingstein, S. P. Harrison, and P. J. Bartlein (2011), Modeling fire and the terrestrial carbon balance, *Global Biogeochem Cy*, *25*, doi: 10.1029/2010gb003906.

Slaughter, C. W. (1983), Summer Shortwave Radiation at a Subarctic Forest Site, *Can J Forest Res*, *13*(5), 740-746.

van der Werf, G. R., J. T. Randerson, L. Giglio, G. J. Collatz, M. Mu, P. S. Kasibhatla, D. C. Morton, R. S. DeFries, Y. Jin, and T. T. van Leeuwen (2010), Global fire emissions and the contribution of deforestation, savanna, forest, agricultural, and peat fires (1997-2009), *Atmos Chem Phys*, *10*(23), 11707-11735, doi: 10.5194/acp-10-11707-2010.

Woodward, F. I., T. M. Smith, and W. R. Emanuel (1995), A Global Land Primary Productivity and Phytogeography Model, *Global Biogeochem Cy*, *9*(4), 471-490.

END OF DOCUMENT